pp 1122–1134.
doi:10.1017/aer.2019.36

Path following of Nano quad-rotors using a novel disturbance observer-enhanced dynamic inversion approach

Yuan Wang
Nanjing University of Aeronautics and Astronautics
Key Laboratory of Fundamental Science for National Defence-Advanced Design Technology of Flight Vehicle,
Nanjing,
China

Xiangming Zheng
zhengxiangming@nuaa.edu.cn
Nanjing University of Aeronautics and Astronautics
Key Laboratory of Fundamental Science for National Defence-Advanced Design Technology of Flight Vehicle,
Nanjing,
China

ABSTRACT

The model of Nano quad-rotors contains many uncertainties such as an external disturbance from a wind field, highly non-linear strong coupling between variables and body measurement errors. To deal with these uncertainties and control the Nano quad-rotors, a novel data-based disturbance observer (DO) is firstly proposed to observe disturbances from a wind field and perturbations from errors of parameter estimation. Then the DO is used to improve the conventional dynamic inversion (DI) method to obtain an enhanced dynamic inversion (EDI) method, which relies only on roughly estimated geometrical parameters, thus eliminating the largest flaw of conventional DI, namely depending on detailed plant information. Simulation results show that the method proposed achieved good trajectory tracking with only roughly estimated geometrical values under wind field; the DO proposed can accurately estimate disturbance from a wind field and perturbation from error of parameter estimation.

Keywords: Nano quad-rotor, Disturbance observer, Dynamic inversion, Path following

Received 31 October 2017; revised 12 April 2018; accepted 18 April 2018.

NOMENCLATURE

I_x, I_y, I_z = roll, pitch and yaw moments of inertial, $kg \cdot m^2$
l = distance between mass point of Nano quad-rotor and rotor, m
m = mass of Nano quad-rotor, Kg
g = gravitational constant, m/s^2
g_1, g_2, g_3 = unknown non-linear terms, rad/s^2
p, q, r = roll, pitch, and yaw rate, rad/s
T_r = thrust of rotors, N
v_x, v_y, v_z = velocity of Nano quad-rotor in inertial coordinate, m/s
w_x, w_y, w_z = wind velocity in inertial coordinate, m/s
x, y, z = position of mass point of Nano quad-rotor in inertial coordinate, m
x_d, y_d, z_d = reference path, m
$\Delta f_p, \Delta f_q, \Delta f_r$ = unmodeled dynamics, rad/s^2
$\Delta f_x, \Delta f_y, \Delta f_z$ = unmodeled dynamics, m/s^2
ϕ, θ, ψ = roll, pitch, and yaw angles, rad
τ_1, τ_2, τ_3 = roll, pitch, and yaw moments, Nm
Φ_p, Φ_q, Φ_r = pseudo gradients for body rate control
$\Phi_{v_x}, \Phi_{v_y}, \Phi_{v_z}$ = pseudo gradients for velocity control
Φ_x, Φ_y, Φ_z = pseudo gradients for position control

1.0 INTRODUCTION

In the past two decades, the dynamic inversion (DI) method has been widely applied in the field of quad-rotor control[1,2]. Compared with conventional methods such as Proportional-Integral-Derivative (PID)[3], linear quadratic regulator (LQR)[4], robust control[5], sliding mode control[6] and back-stepping control[7], it is simple in control scheme and easy in parameter tuning; however, it demands an accurate model of aircraft, which is its largest flaw and the reason for its poor robustness[8]. Nano quad-rotors have a low in-flight speed, and are light in weight and limited in thrust; thus, they are susceptible to external disturbances (such as from wind field) and internal disturbances (such as unmodeled dynamics and perturbation of measurable parameters). Therefore, it is difficult, or even impossible, to obtain their accurate model, resulting in poor body stability and flight performance. Targeting the flight of quad-rotors (including regular-sized and Nano-sized) in a wind field and under parameter perturbations, many studies have been carried out. For example, the active disturbance rejection control (ADRC), which uses extended state observer (a DO) to observe disturbances that can be modelled, was used in the design of attitude system control[9,10] but it shows deficiency in estimation of disturbances that cannot be modelled[11], such as a turbulent wind field. In addition, parameter tuning of ADRC-based controllers are not convenient. For another example, robust control is used to deal with small disturbances encountered by quad-rotors in flight[5], but research on the Nano quad-rotors in flight under disturbances is quite limited.

It can be seen from the above analysis that a good flight controller should have good performance in dealing with internal and external disturbances; therefore, a disturbance observer (DO) is adopted to enhance the conventional DI method and improve the system robustness of Nano quad-rotors. First, a novel data-based DO, which can only use rough model information to estimate disturbances (including internal and external disturbances and non-linear terms affecting model accuracy) of control system, is proposed to eliminate the accurate model dependency of the conventional DI method and significantly improve system robustness of the DI method. Secondly, the stability of the DO proposed is verified. Finally, the proposed

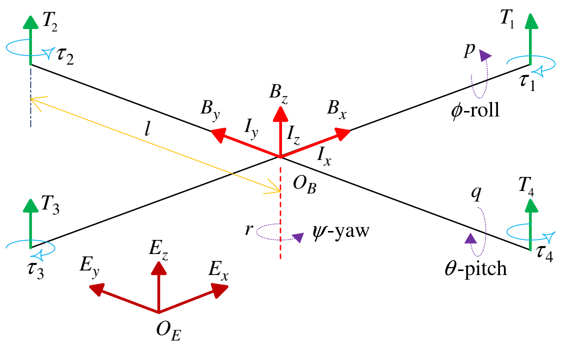

Figure 1. Preliminary knowledge of quad-rotors.

DO is integrated into the conventional DI method to replace the accurately modelled terms with disturbance terms observed by the DO for design of control scheme. Simulation results show that the EDI method, which does not rely on an accurate model of the quad-rotors, realises good performance in tracking a given path under a wind field. It is demonstrated that the proposed DO can accurately estimate both disturbances that cannot be modelled, such as a wind field and disturbances that can be modelled due to error in parameter estimation.

2.0 MODEL OF NANO QUAD-ROTORS SUBJECT TO DISTURBANCES

Two main coordinates, some forces, moments and geometrical parameters are introduced first before modelling Nano quad-rotors, as shown in Fig. 1,

In Fig. 1, $O_E E_x E_y E_z$ represents the inertial coordinate, in which E_x and E_y are on the horizontal plane and E_x is perpendicular to E_y, and E_z is perpendicular to the horizontal determined by right-hand rule. $O_B B_x B_y B_z$ represents the body coordinate whose origin is fixed at the centre of gravity of the quad-rotor. B_x is the normal flight orientation, B_y is positive to starboard in the horizontal plane and B_z is orthogonal to the plane $B_x O_B B_y$.

The non-linear equations of motion subject to disturbances for Nano quad-rotors[12] are expressed as:

$$\begin{cases} \dot{x} = v_x + w_x \\ \dot{y} = v_y + w_y \\ \dot{z} = v_z + w_z \end{cases}, \quad \begin{cases} \dot{v}_x = (\cos\phi\sin\theta\cos\psi + \sin\phi\sin\psi)\frac{T_r}{m} + \Delta f_x \\ \dot{v}_y = (\cos\phi\sin\theta\sin\psi - \sin\phi\cos\psi)\frac{T_r}{m} + \Delta f_y \\ \dot{v}_z = -g + \frac{T_r}{m}\cos\phi\cos\theta + \Delta f_z \end{cases},$$

$$\begin{cases} \dot{\phi} = p + q\sin\phi\tan\theta + r\cos\phi\tan\theta \\ \dot{\theta} = q\cos\phi - r\sin\phi \\ \dot{\psi} = q\sin\phi\sec\theta + r\cos\phi\sec\theta \end{cases}, \quad \begin{cases} \dot{p} = \underbrace{\frac{I_y - I_z}{I_x}qr + \Delta f_p + \left(\frac{l}{I_x} - b_1\right)\tau_1}_{g_1(p,q,r;t)} + b_1 u_1 \\ \dot{q} = \underbrace{\frac{I_z - I_x}{I_y}pr + \Delta f_q + \left(\frac{l}{I_y} - b_2\right)\tau_2}_{g_2(p,q,r;t)} + b_2 u_2 \\ \dot{r} = \underbrace{\frac{I_x - I_y}{I_z}pq + \Delta f_r + \left(\frac{1}{I_z} - b_3\right)\tau_3}_{g_3(p,q,r;t)} + b_3 u_3 \end{cases} \quad \ldots (1)$$

https://doi.org/10.1017/aer.2019.36 Published online by Cambridge University Press

Equation (1) is formed by four equation sets in which the first set represents translational kinematics (position control), the second set represents translational dynamics (velocity control), the third set represents rotational kinematics (Euler angle control) and the fourth set represents rotational dynamics (body rate control). In the above, $[x, y, z]^T$ and $[v_x, v_y, v_z]^T \in R^3$ represent position and velocity vectors in inertial frame, respectively. m and g represent mass and gravitational constant, respectively. $[p, q, r]^T \in R^3$ is the angular velocity vector under body coordinate system. $[\phi, \theta, \psi]^T \in R^3$ is the Euler angle under inertial coordinate system. T_r is lift and $[u_2, u_3, u_4]^T$ represents virtual inputs (roll force, pitch force and yaw moment) acting on quad-rotors. I_x, I_y, I_z are moments of inertial. w_x, w_y and w_z represent wind velocity in inertial frame along the x, y and z axes, respectively. Δf_x, Δf_y, Δf_z, Δf_p, Δf_q and Δf_r are unmodeled dynamics. b_1, b_2 and b_3 are estimations of l/I_x , l/I_y and $1/I_z$, respectively.

3.0 DISTURBANCE OBSERVER DESIGN FOR AN AFFINE NON-LINEAR SYSTEM

3.1 Design procedure

Consider the commonly used first-order affine non-linear system with disturbance, shown as:

$$\Sigma_1 : \dot{y} = f(y, t) + b(y, t) \cdot u(t) + d(t) \qquad \ldots (2)$$

where, $f(*)$ and $b(*)$ are unknown, and $d(t)$ includes internal and external disturbances. $u(t)$ and y are measurable variables, representing input and output, respectively.

A discretising system Σ_1 with the sampling time period T yields:

$$y(k+1) = y(k) + T \cdot [f(y(k), t(k)) + b(y(k), t(k)) \cdot u(k) + d(t(k))] \qquad \ldots (3)$$

Select a reference model with a discretised formation as:

$$y_m(k+1) = y_m(k) + T \cdot b_m \cdot u(k) \qquad \ldots (4)$$

where, the gain b_m is given. The rest of the work is to estimate $g(y(k), u(k); t(k)) = f(y(k), t(k)) + (b(y(k), t(k)) - b_m)u(k) + d(t(k))$ by designing a DO using input and output data.

Taking the notation $e(k) = y(k) - y_m(k)$ and subtracting Equation (4) from (3) yields a new non-linear system:

$$\Sigma_2 : \ \Delta e(k+1) = T \cdot g(y(k), u(k); t(k)) \qquad \ldots (5)$$

Then at k^{th} sampling time point:

$$\Delta e(k) = T \cdot g(y(k-1), u(k-1); t(k-1)) \qquad \ldots (6)$$

Subtracting Equation (6) from (5) yields:

$$\Delta e(k+1) = \Delta e(k) + \Delta g(y(k), u(k); t(k)) \qquad \ldots (7)$$

https://doi.org/10.1017/aer.2019.36 Published online by Cambridge University Press

Reference[13] introduces a non-linear discrete system written as:

$$\Sigma_0: \ y(k+1) = f(y(k), \cdots, y(k-n_y), u(k), \cdots, u(k-n_u)) \qquad \ldots (8)$$

can be linearized into the following formation by using dynamic linearization (DL) theory:

$$\triangle y(k+1) = \Phi^T(k)\, \triangle H(k) \qquad \ldots (9)$$

where, $u(k) \in R$ and $y(k) \in R$ represent input and output of the system, respectively. n_y and n_u are two integers. $f(*): R^{n_y+n_u+2} \mapsto R$ is a non-linear mapping. $\Phi(k) = [\phi_1(k), \cdots \phi_{L_y}(k), \phi_{L_y+1}(k), \cdots, \phi_{L_y+L_u}(k)]^T \in R^{L_y+L_u}$ is a time-varying vector called pseudo gradient (PG), and $\|\Phi(k)\| \leq b$, L_y and $L_u (0 \leq L_y \leq n_y, 1 \leq L_u \leq n_u)$ are integers called pseudo order (PO). $\triangle y(k) = y(k) - y(k-1)$, $\triangle u(k) = u(k) - u(k-1)$ and $\triangle H(k) = H(k) - H(k-1) = \left[\triangle y(k), \cdots \triangle y(k-L_y+1), \triangle u(k), \cdots \triangle u(k-L_u+1)\right]^T$.

Applying DL theory to a linearize system Σ_2 yields:

$$\Sigma_2: \ \Delta e(k+1) = \Delta e(k) + T \cdot \Phi(k) \cdot \Delta H(k) \qquad \ldots (10)$$

where, $\triangle H(k) = \left[\triangle e(k), \cdots \triangle e(k-L_y+1), \triangle u(k), \cdots \triangle u(k-L_u+1)\right]^T$.

Thus, finally, by making a comparison with Equation (7) and (10), the disturbance term can be estimated as:

$$g(y(k), u(k); t(k)) = \frac{\Delta e(k)}{T} + \Phi(k) \cdot \Delta H(k) \qquad \ldots (11)$$

It can be seen that only $\Phi(k)$ needs to be updated online. By using the following cost function:

$$J(\underline{\Phi}(k)) = \left|y(k) - y(k-1) - \underline{\Phi}^T(k)\, \triangle H(k-1)\right|^2 + \mu \left\|\underline{\Phi}(k) - \underline{\Phi}(k-1)\right\|^2 \qquad \ldots (12)$$

and letting $\frac{\partial J(\underline{\Phi}(k))}{\partial \underline{\Phi}(k)} = 0$, the PG $\underline{\Phi}(k)$ can be updated online as:

$$\underline{\Phi}(k) = \underline{\Phi}(k-1) + \frac{\gamma\, \triangle H(k) \left[y(k) - y(k-1) - \underline{\Phi}^T(k-1)\, \triangle H(k-1)\right]}{\mu + \|\triangle H(k-1)\|^2} \qquad \ldots (13)$$

where, $\gamma \in (0, 2]$, $\mu > 0$ and $\underline{\Phi}(k)$ is the estimation of $\Phi(k)$. In the next section, $\underline{\Xi}$ represents the estimation of Ξ.

3.2 Convergence analysis

This part aims to prove the boundedness of the error between $\Phi(k)$ and $\underline{\Phi}(k)$. Subtracting the real value $\Phi(k)$ from both sides of Equation (13) and denoting $\underline{\underline{\Phi}}(k) = \underline{\Phi}(k) - \Phi(k)$ yields:

$$\underline{\underline{\Phi}}(k) = \left[I - \frac{\gamma \cdot \Delta H(k-1) \cdot \Delta H^T(k-1)}{\mu + \|\Delta H(k-1)\|^2}\right] \underline{\underline{\Phi}}(k-1) + \Phi(k-1) - \Phi(k) \qquad \ldots (14)$$

where, I is an identity matrix.

Taking the norm of both sides of Equation (14) yields:

$$\left\|\underline{\underline{\Phi}}(k)\right\| \leq \left\|\left[I - \frac{\gamma \cdot \Delta H(k-1) \cdot \Delta H^T(k-1)}{\mu + \|\Delta H(k-1)\|^2}\right]\underline{\underline{\Phi}}(k-1)\right\| + \|\Phi(k-1) - \Phi(k)\|$$
$$\leq \left\|\left[I - \frac{\gamma \cdot \Delta H(k-1) \cdot \Delta H^T(k-1)}{\mu + \|\Delta H(k-1)\|^2}\right]\underline{\underline{\Phi}}(k-1)\right\| + 2b \quad (15)$$

Since

$$\left\|\left[I - \frac{\gamma \cdot \Delta H(k-1) \cdot \Delta H^T(k-1)}{\mu + \|\Delta H(k-1)\|^2}\right]\underline{\underline{\Phi}}(k-1)\right\|^2 \leq \left\|\underline{\underline{\Phi}}(k-1)\right\|^2$$
$$+ \left[-2 + \frac{\gamma \cdot \|\Delta H(k-1)\|^2}{\mu + \|\Delta H(k-1)\|^2}\right] \cdot \frac{\gamma\left[\underline{\underline{\Phi}}^T(k-1)\Delta H(k-1)\right]^2}{\mu + \|\Delta H(k-1)\|^2} \quad (16)$$

Based on $\gamma \in (0, 2]$ and $\mu > 0$, the following inequality works:

$$-2 + \frac{\gamma \cdot \|\Delta H(k-1)\|^2}{\mu + \|\Delta H(k-1)\|^2} < 0 \quad \ldots (17)$$

Thus:

$$\left\|\left[I - \frac{\gamma \cdot \Delta H(k-1) \cdot \Delta H^T(k-1)}{\mu + \|\Delta H(k-1)\|^2}\right]\underline{\underline{\Phi}}(k-1)\right\| \leq \xi \left\|\underline{\underline{\Phi}}(k-1)\right\| \quad \ldots (18)$$

where, $0 < \xi < 1$. Finally, the following relationship works:

$$\left\|\underline{\underline{\Phi}}(k)\right\| \leq \xi \left\|\underline{\underline{\Phi}}(k-1)\right\| + 2b \leq \xi^2 \left\|\underline{\underline{\Phi}}(k-2)\right\|$$
$$+ 2\xi b + 2b \leq \cdots \leq \xi^{k-1} \left\|\underline{\underline{\Phi}}(1)\right\| + \frac{2b(1-\xi^{k-1})}{1-\xi} \quad (19)$$

Thus, error convergence of the proposed DO is proved.

4.0 CONTROL SCHEME

Since all states in a Nano quad-rotor system are observable and measurable, the reference model can be selected as:

$$\begin{cases} \dot{x}_m = v_{xm} \\ \dot{v}_{xm} = \underbrace{(\cos\phi \sin\theta \cos\psi + \sin\phi \sin\psi)\frac{T_r}{m}}_{\xi_x} \end{cases}, \quad \begin{cases} \dot{y}_m = v_{ym} \\ \dot{v}_{ym} = \underbrace{(\cos\phi \sin\theta \sin\psi - \sin\phi \cos\psi)\frac{T_r}{m}}_{\xi_y} \end{cases},$$
$$\begin{cases} \dot{z}_m = v_{zm} \\ \dot{v}_{zm} = \underbrace{-g + \frac{T_r}{m}\cos\phi \cos\theta}_{\xi_z} \end{cases}, \quad \begin{cases} \dot{p}_m = b_1 u_2 \\ \dot{q}_m = b_2 u_3 \\ \dot{r}_m = b_3 u_4 \end{cases} \quad \ldots (20)$$

https://doi.org/10.1017/aer.2019.36 Published online by Cambridge University Press

Thus, the wind velocities and unmodeled dynamics can be observed using the DO proposed as shown in Table 1:

Based on the estimations of disturbances, the position control scheme is:

$$x\,control:\begin{cases}\dot{x}_c=\omega_1(x_c-x)\\ v_{xc}=\dot{x}_c-\underline{w}_x\\ \dot{v}_{xc}=\omega_2(v_{xc}-v_x)\\ \xi_x=\dot{v}_{xc}-\Delta\underline{f}_x\end{cases},\quad y\,control:\begin{cases}\dot{y}_c=\omega_1(y_c-y)\\ v_{yc}=\dot{y}_c-\underline{w}_y\\ \dot{v}_{yc}=\omega_2(v_{yc}-v_y)\\ \xi_y=\dot{v}_{yc}-\Delta\underline{f}_y\end{cases},\quad z\,control:\begin{cases}\dot{z}_c=\omega_1(z_c-z)\\ v_{zc}=\dot{z}_c-\underline{w}_z\\ \dot{v}_{zc}=\omega_2(v_{zc}-v_z)\\ \xi_z=\dot{v}_{zc}-\Delta\underline{f}_z\end{cases}\quad \ldots(21)$$

where, x_c, y_c and z_c represent the reference path. v_{xc}, v_{yc} and v_{zc} are command translational velocity. ω_1 and ω_2 are controller parameters. By commanding the desired yaw angle, the desired Euler angle and thrust can be solved by following equations:

$$\begin{cases}\psi_c=Commanded\ \ value\\ \phi_c=\arcsin\left(\frac{\xi_x\sin\psi_c-\xi_y\cos\psi_c}{\sqrt{\xi_x^2+\xi_y^2+(\xi_z+g)^2}}\right)\\ \theta_c=\arctan\left(\frac{\xi_x\cos\psi_c+\xi_y\sin\psi_c}{\xi_z+g}\right)\\ T_r=m[\xi_x\,(\cos\phi_c\sin\theta_c\cos\psi_c+\sin\phi_c\sin\psi_c)\\ \qquad+\xi_y(\cos\phi_c\sin\theta_c\sin\psi_c-\sin\phi_c\cos\psi_c)+(\xi_z+g)\cos\phi_c\cos\theta_c]\end{cases}\quad \ldots(22)$$

and the attitude control scheme is:

$$Roll\ rate:\begin{cases}p_c=\omega_3(\phi_c-\phi)\\ \dot{p}_c=\omega_4(p_c-p)\\ u_2=\frac{1}{b_1}(\dot{p}_c-\underline{g}_1)\end{cases},\quad Pitch\ rate:\begin{cases}q_c=\omega_3(\theta_c-\theta)\\ \dot{q}_c=\omega_4(q_c-q)\\ u_3=\frac{1}{b_2}(\dot{q}_c-\underline{g}_2)\end{cases},\quad Yaw\ rate:\begin{cases}r_c=\omega_3(\psi_c-\psi)\\ \dot{r}_c=\omega_4(r_c-r)\\ u_4=\frac{1}{b_3}(\dot{r}_c-\underline{g}_3)\end{cases}\quad \ldots(23)$$

In above equation, ϕ_c, θ_c and ψ_c are command Euler angle. p_c, q_c and r_c are command body rate. ω_3 and ω_4 are controller parameters.

5.0 NUMERICAL VALIDATION

In this part, a numerical simulation was conducted to verify the proposed control scheme. The parameters[14] of the Nano quad-rotor used here are: $m=0.04389kg$, $l=0.035m$, $I_x=I_y=1.916\times10^{-5}$ and $I_z=2.781\times10^{-5}$.

The Dryden model[11] is adopted to generate the wind field in which the steady wind velocities along the x, y and z axes in the earth frame are assumed to be 1 m/s. To show that the path following the Nano quad-rotor does not depend on the detailed model information, we assume that the three parameters b_1, b_2 and b_3 perturb within a wide area, in order to show that the Nano quad-rotor does not depend on the detailed model information when it does path following task $-30\%\sim+0.5m$. Meanwhile, an additional mass with the weight $50\%m$ is added on the Nano quad-rotor.

The parameters in above scheme are:

$\omega_1=2$, $\omega_2=4$, $\omega_3=6$ and $\omega_4=30$. The relationships $\omega_4=n_1\omega_3, \omega_2=n_2\omega_1$, $n_i=2\sim5$, $i=1,2$ work according to the response speed (body rate $p,q,r>$ Euler angle $\phi,\theta,\psi>$ translational velocity $v_x,v_y,v_z>$ position x,y,z) of the quad-rotor system.

https://doi.org/10.1017/aer.2019.36 Published online by Cambridge University Press

Table 1
Disturbance observers design for Nano quad-rotor control system

Disturbance term	PG online updating
$\underline{w}_x(k) = \dfrac{\Delta e_x(k)}{T} + \underline{\Phi}_x(k) \cdot \Delta H_x(k)$	$\underline{\Phi}_x(k) = \underline{\Phi}_x(k-1) + \dfrac{\gamma_x \triangle H_x(k)\left[e_x(k) - e_x(k-1) - \underline{\Phi}_x^T(k-1) \triangle H_x(k-1)\right]}{\mu_x + \Vert \triangle H_x(k-1)\Vert^2}$ $e_x(k) = x(k) - x_m(k)$ $\triangle H_x(k) = \left[\triangle e_x(k), \cdots \triangle e_x(k - L_{yx} + 1), \triangle v_x(k), \cdots \triangle v_x(k - L_{ux} + 1)\right]^T$
$\underline{w}_y(k) = \dfrac{\Delta e_y(k)}{T} + \underline{\Phi}_y(k) \cdot \Delta H_y(k)$	$\underline{\Phi}_y(k) = \underline{\Phi}_y(k-1) + \dfrac{\gamma_y \triangle H_y(k)\left[e_y(k) - e_y(k-1) - \underline{\Phi}_y^T(k-1) \triangle H_y(k-1)\right]}{\mu_y + \left\Vert \triangle H_y(k-1)\right\Vert^2}$ $e_y(k) = y(k) - y_m(k)$ $\triangle H_y(k) = \left[\triangle e_y(k), \cdots \triangle e_y(k - L_{yy} + 1), \triangle v_y(k), \cdots \triangle v_y(k - L_{uy} + 1)\right]^T$
$\underline{w}_z(k) = \dfrac{\Delta e_z(k)}{T} + \underline{\Phi}_z(k) \cdot \Delta H_z(k)$	$\underline{\Phi}_z(k) = \underline{\Phi}_z(k-1) + \dfrac{\gamma_z \triangle H_z(k)\left[e_z(k) - e_z(k-1) - \underline{\Phi}_z^T(k-1) \triangle H_z(k-1)\right]}{\mu_z + \Vert \triangle H_z(k-1)\Vert^2}$ $e_z(k) = z(k) - z_m(k)$ $\triangle H_z(k) = \left[\triangle e_z(k), \cdots \triangle e_z(k - L_{yz} + 1), \triangle v_z(k), \cdots \triangle v_z(k - L_{uz} + 1)\right]^T$
$\Delta \underline{f}_x(k) = \dfrac{\Delta e_{v_x}(k)}{T} + \underline{\Phi}_{v_x}(k) \cdot \Delta H_{v_x}(k)$	$\underline{\Phi}_{v_x}(k) = \underline{\Phi}_{v_x}(k-1) + \dfrac{\gamma_{v_x} \triangle H_{v_x}(k)\left[e_{v_x}(k) - e_{v_x}(k-1) - \underline{\Phi}_{v_x}^T(k-1) \triangle H_{v_x}(k-1)\right]}{\mu_{v_x} + \left\Vert \triangle H_{v_x}(k-1)\right\Vert^2}$ $e_{v_x}(k) = v_x(k) - v_{xm}(k)$ $\triangle H_{v_x}(k) = \left[\triangle e_{v_x}(k), \cdots \triangle e_{v_x}(k - L_{yv_x} + 1), \triangle \xi_x(k), \cdots \triangle \xi_x(k - L_{uv_x} + 1)\right]^T$
$\Delta \underline{f}_y(k) = \dfrac{\Delta e_{v_y}(k)}{T} + \underline{\Phi}_{v_y}(k) \cdot \Delta H_{v_y}(k)$	$\underline{\Phi}_{v_y}(k) = \underline{\Phi}_{v_y}(k-1) + \dfrac{\gamma_{v_y} \triangle H_{v_y}(k)\left[e_{v_y}(k) - e_{v_y}(k-1) - \underline{\Phi}_{v_y}^T(k-1) \triangle H_{v_y}(k-1)\right]}{\mu_{v_y} + \left\Vert \triangle H_{v_y}(k-1)\right\Vert^2}$ $e_{v_y}(k) = v_y(k) - v_{ym}(k)$ $\triangle H_{v_y}(k) = \left[\triangle e_{v_y}(k), \cdots \triangle e_{v_y}(k - L_{yv_y} + 1), \triangle \xi_y(k), \cdots \triangle \xi_y(k - L_{uv_y} + 1)\right]^T$
$\Delta \underline{f}_z(k) = \dfrac{\Delta e_{v_z}(k)}{T} + \underline{\Phi}_{v_z}(k) \cdot \Delta H_{v_z}(k)$	$\underline{\Phi}_{v_z}(k) = \underline{\Phi}_{v_z}(k-1) + \dfrac{\gamma_{v_z} \triangle H_{v_z}(k)\left[e_{v_z}(k) - e_{v_z}(k-1) - \underline{\Phi}_{v_z}^T(k-1) \triangle H_{v_z}(k-1)\right]}{\mu_{v_z} + \left\Vert \triangle H_{v_z}(k-1)\right\Vert^2}$ $e_{v_z}(k) = v_z(k) - v_{zm}(k)$ $\triangle H_{v_z}(k) = \left[\triangle e_{v_z}(k), \cdots \triangle e_{v_z}(k - L_{yv_z} + 1), \triangle \xi_z(k), \cdots \triangle \xi_z(k - L_{uv_z} + 1)\right]^T$
$\underline{g}_1(k) = \dfrac{\Delta e_p(k)}{T} + \underline{\Phi}_p(k) \cdot \Delta H_p(k)$	$\underline{\Phi}_p(k) = \underline{\Phi}_p(k-1) + \dfrac{\gamma_p \triangle H_p(k)\left[e_p(k) - e_p(k-1) - \underline{\Phi}_p^T(k-1) \triangle H_p(k-1)\right]}{\mu_p + \left\Vert \triangle H_p(k-1)\right\Vert^2}$ $e_p(k) = p(k) - p_m(k)$ $\triangle H_p(k) = \left[\triangle e_p(k), \cdots \triangle e_p(k - L_{yp} + 1), \triangle \tau_1(k), \cdots \triangle \tau_1(k - L_{up} + 1)\right]^T$
$\underline{g}_2(k) = \dfrac{\Delta e_q(k)}{T} + \underline{\Phi}_q(k) \cdot \Delta H_q(k)$	$\underline{\Phi}_q(k) = \underline{\Phi}_q(k-1) + \dfrac{\gamma_q \triangle H_q(k)\left[e_q(k) - e_q(k-1) - \underline{\Phi}_p^T(k-1) \triangle H_q(k-1)\right]}{\mu_q + \left\Vert \triangle H_q(k-1)\right\Vert^2}$ $e_q(k) = q(k) - q_m(k)$ $\triangle H_q(k) = \left[\triangle e_q(k), \cdots \triangle e_q(k - L_{yq} + 1), \triangle \tau_2(k), \cdots \triangle \tau_2(k - L_{uq} + 1)\right]^T$
$\underline{g}_3(k) = \dfrac{\Delta e_r(k)}{T} + \underline{\Phi}_r(k) \cdot \Delta H_r(k)$	$\underline{\Phi}_r(k) = \underline{\Phi}_r(k-1) + \dfrac{\gamma_r \triangle H_r(k)\left[e_r(k) - e_r(k-1) - \underline{\Phi}_r^T(k-1) \triangle H_r(k-1)\right]}{\mu_r + \Vert \triangle H_r(k-1)\Vert^2}$ $e_r(k) = r(k) - r_m(k)$ $\triangle H_r(k) = \left[\triangle e_r(k), \cdots \triangle e_r(k - L_{yr} + 1), \triangle \tau_3(k), \cdots \triangle \tau_3(k - L_{ur} + 1)\right]^T$

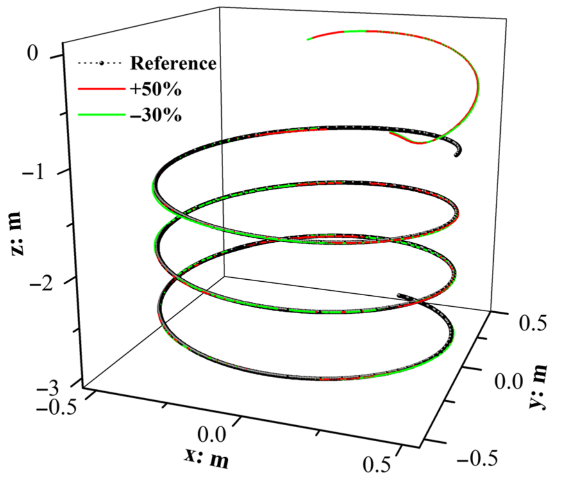

Figure 2. Effect of 3D path following.

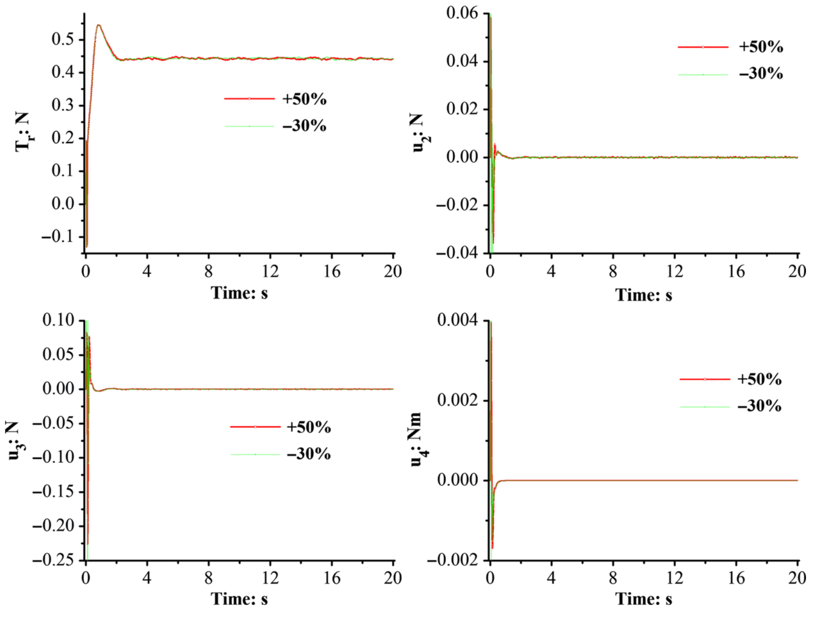

Figure 3. Virtual inputs.

$\gamma_x = \gamma_y = \gamma_z = 1$, $\gamma_{v_x} = \gamma_{v_y} = \gamma_{v_z} = 1$, $\gamma_p = \gamma_q = \gamma_r = 1$, $\mu_x = \mu_y = \mu_z = 1$, $\mu_{v_x} = \mu_{v_y} = \mu_{v_z} = 1$ and $\mu_p = \mu_q = \mu_r = 1$. They satisfy the conditions $\gamma \in (0, 2]$ and $\mu > 0$ mentioned in Section 3.2.

$L_{yx} = L_{yy} = L_{yz} = 0$, $L_{yv_x} = L_{yv_y} = L_{yv_z} = 0$, $L_{yp} = L_{yq} = L_{yr} = 0$, $L_{ux} = L_{uy} = L_{uz} = 1$, $L_{uv_x} = L_{uv_y} = L_{uv_z} = 1$ and $L_{up} = L_{uq} = L_{ur} = 1$. These parameters control the linearized length of the quad-rotor system. Other values are also applicable.

The reference signal is:

https://doi.org/10.1017/aer.2019.36 Published online by Cambridge University Press

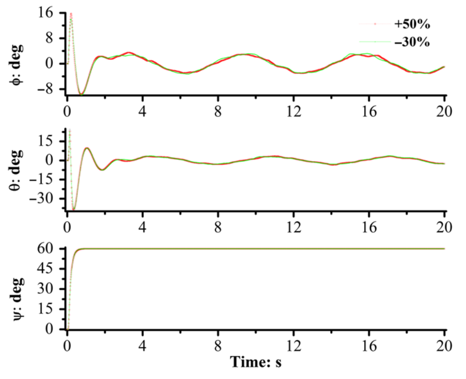

Figure 4. Euler angle.

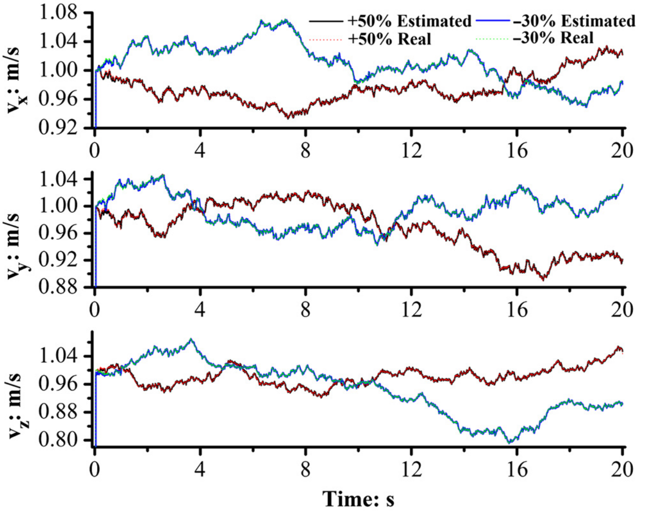

Figure 5. Estimation of w_x, w_y and w_z.

$$x_c(t) = \frac{1}{2}\cos t\ (m),\ \ y_c(t) = \frac{1}{2}\sin t\ (m),\ \ z_c(t) = -1 - \frac{t}{10}\ (m),\ \ \psi_c(t) = \frac{\pi}{3}\ (rad) \quad \ldots (24)$$

Simulation results are shown as in Fig. 2–Fig. 9:

It is clearly shown in Fig. 2–Fig. 4 that the EDI-based method achieves good performance under the wind field without using an accurate model, bringing a satisfactory response time. In Figs. 5–9, the proposed DO accurately estimates not only the disturbances that can be modelled, but also the coloured noise. In the Dryden wind field model, the wind is actually the steady wind adding turbulence (simulated using coloured noise converted from a standard Gaussian white noise signal passing through forming filter); thus, in fact, the disturbance is not time continuous. Since the disturbance estimation in the DO proposed in this paper is based on the differences between plant model and reference model, the characteristics of the disturbance are not strictly assumed.

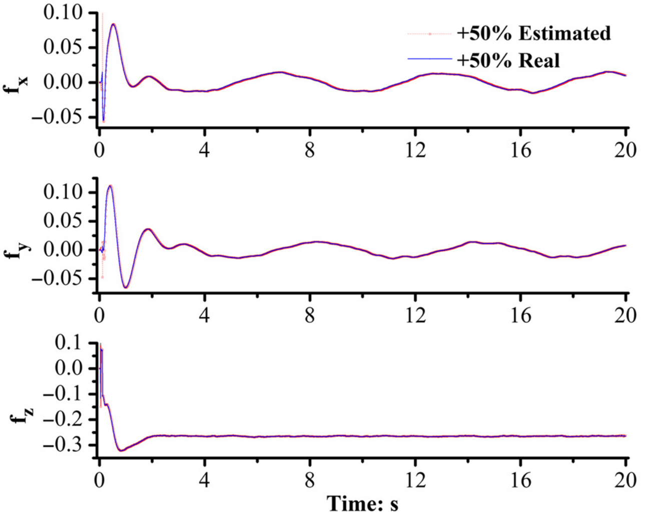

Figure 6. Estimation of f_x, f_y and f_z: +50% perturbation.

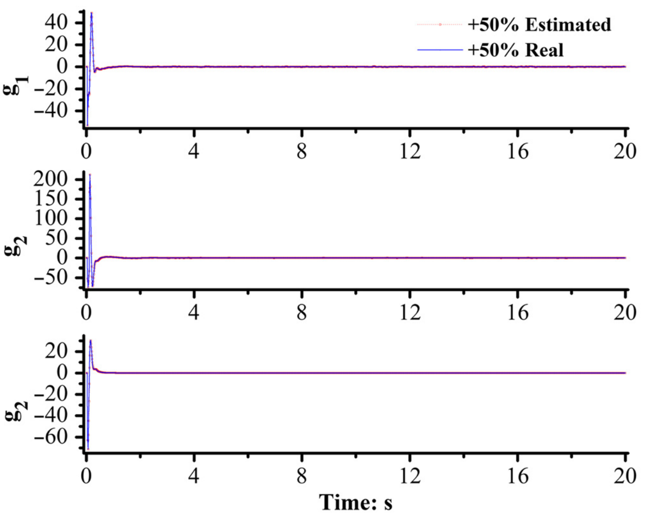

Figure 7. Estimation of g_1, g_2 and g_3: +50% perturbation.

6.0 CONCLUSIONS

An EDI method that eliminates detailed model dependency, which is the largest flaw of conventional DI method, is proposed for trajectory tracking and control of Nano quad-rotors. Firstly, for a measurable and observable system, a novel data-based DO is proposed to estimate both disturbances that cannot be modelled, such as a wind field and disturbances that can be modelled due to error in parameter estimation. Secondly, the stability of the proposed DO

https://doi.org/10.1017/aer.2019.36 Published online by Cambridge University Press

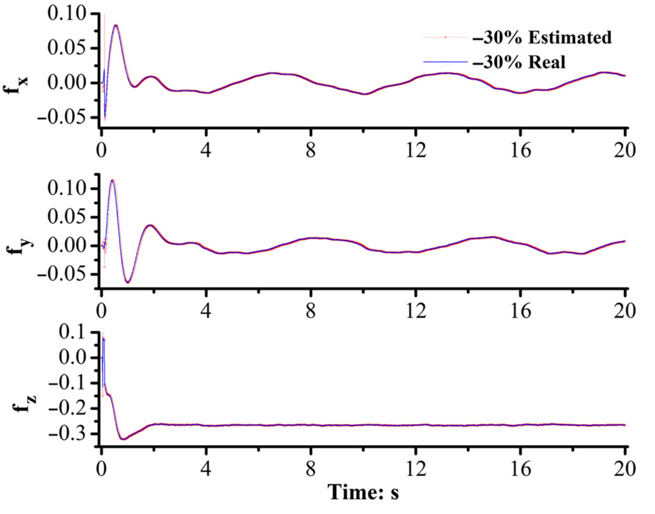

Figure 8. Estimation of f_x, f_y and f_z: −30% perturbation.

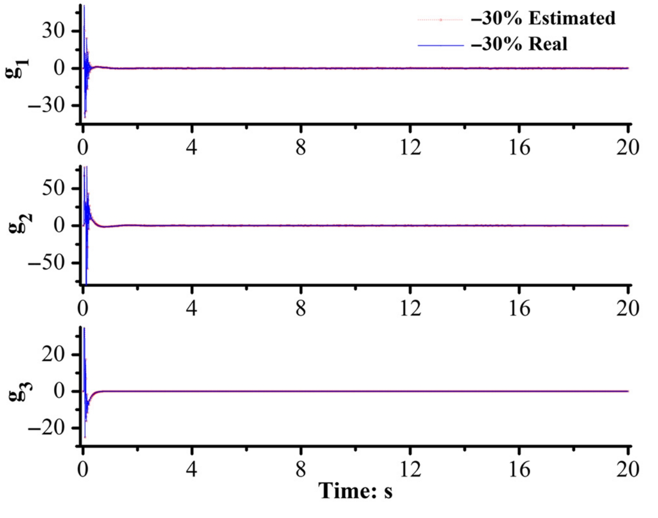

Figure 9. Estimation of g_1, g_2 and g_3: −30% perturbation.

is verified. Finally, the proposed DO is adopted to enhance the DI method for better robustness. Simulation results show that, even with the relatively large error in the estimation of model parameters and under disturbances from a wind field, the enhanced DI method can realise trajectory tracking and control of Nano quad-rotors.

https://doi.org/10.1017/aer.2019.36 Published online by Cambridge University Press

ACKNOWLEDGEMENTS

This publication was supported by the Priority Academic Program Development of Jiangsu Higher Education Institutions.

REFERENCES

1. LIN, Q., CAI, Z.H., WANG, Y.X., YANG, J.P. and CHEN, L.F. Adaptive flight control design for quadrotor UAV based on dynamic inversion and neural networks, Third International Conference on Instrumentation, Measurement, Computer, Communication and Control, IEEE, 2014, Shenyang, China, pp 1461–1466. doi:10.1109/ IMCCC.2013.326.
2. DAS, A., SUBBARAO, K. and LEWIS, F. Dynamic inversion with zero-dynamics stabilisation for quadrotor control, *IET Control Theory & Applications*, 2009, **3**, (3), pp 303–314. doi:10.1049/iet-cta:20080002.
3. SÁ, R.C., ARAÚJO, A.L.C.D., VARELA, A.T. and BARRETO, G.D.A. Construction and PID control for stability of an unmanned aerial vehicle of the type quadrotor, Robotics Symposium and Competition, IEEE, 2013, **10**, Arequipa, Peru, pp 95–99. doi:10.1109/LARS.2013.64.
4. BOUABDALLAH, S., NOTH, A. and SIEGWART, R. PID vs LQ control techniques applied to an indoor micro quadrotor, RSJ International Conference on Intelligent Robots and Systems, IEEE, 2004, **3**, Sendai, Japan, pp 2451–2456. doi:10.1109/IROS.2004.1389776.
5. ISLAM, S., FARAZ, M., ASHOUR, R.K., DIAS, J. and SENEVIRATNE, L.D. Robust adaptive control of quadrotor unmanned aerial vehicle with uncertainty, International Conference on Robotics and Automation, IEEE, 2015, Seattle, WA, USA, pp 1704–1709. doi:10.1109/ICRA.2015.7139417.
6. FAN, Y., CAO, Y. and ZHAO, Y. Sliding mode control for nonlinear trajectory tracking of a quadrotor, Chinese Control Conference (CCC), IEEE, 2017, Dalian, China, pp 6676–6680. doi:10.23919/ChiCC.2017.8028413.
7. MADANI, T. and BENALLEGUE, A. Control of a quadrotor mini-helicopter via full state backstepping technique, Proceedings of the IEEE Conference on Decision and Control, IEEE, 2007, San Diego, CA, USA, pp 1515–1520. doi:10.1109/CDC.2006.377548.
8. SCHUMACHER, C. and KHARGONEKAR, P.P. Missile autopilot designs using H1 control with gain scheduling and dynamic inversion, *J Guidance, Control, and Dynamics*, 1998, **21**, (2), pp 234–243. doi:10.2514/2.4248.
9. YE, B., LAN, W., JIN, H. and HUANG, C. Linear active disturbance rejection control of quadrotor's altitude and attitude, Automation, IEEE, 2017, pp 1188–1193. doi:10.1109/YAC.2017.7967593.
10. LIBO, Q., WENYA, Z., LONG'EN, L. and WENHUI, J. Active disturbance rejection control system design for quadrotor, Chinese Control Conference (CCC), IEEE, 2017, Dalian, China, pp 6530–6534. doi:10.23919/ChiCC.2017.8028413.
11. BEARD, R.W. and MCLAIN, T.W. *Small unmanned aircraft: Theory and practice*, Princeton University Press, 2012, New Jersey.
12. DERAFA, L., OULDALI, A., MADANI, T. and BENALLEGUE, A. Non-linear control algorithm for the four rotors UAV attitude tracking problem, *Aeronautical J*, 2011, **115**, (1165), pp 175–185. doi:10.1017/S0001924000005571.
13. HOU, Z., CHI, R. and GAO, H. An overview of dynamic-linearization-based data-driven control and applications, *IEEE Transactions Industrial Electronics*, **64**, (5), 2017, pp 4076–4090. doi:10.1109/TIE.2016.2636126.
14. LI, X. and CHEN, M. Extended state observer-based nonlinear cascade proportional-integral–derivative control of the Nano quadrotor, *Advances in Mechanical Engineering* 2016, **8**, (12), 1687814016680799. doi:10.1177/1687814016680799.